In-Situ Control of Tunable Evanescent-Mode Cavity Filters Using Differential Mode Monitoring

Hjalti H. Sigmarsson, Andrew Christianson, Himanshu Joshi,
Sungwook Moon, Dimitrios Peroulis, and William J. Chappell

Department of Electrical and Computer Engineering, Birck Nanotechnology Center,
Purdue University, West Lafayette, Indiana, 47907, USA

***Abstract* — In the present work, a method for tracking the center frequency of a widely tunable evanescent-mode cavity filter in-situ is introduced. The goal is to be able to monitor the performance of a filter without disturbing the fields or degrading the quality. The proposed method is to monitor the resonant frequency of each resonator of the filter independently by inducing higher order differential modes. This method enables a continuous feedback loop to lock in the filter center frequency and shape. An example filter is fabricated to demonstrate the concept and tuned from 1.4 to 3 GHz while monitoring the differential mode at 4 to 6.5 GHz. The ability to independently monitor and control the individual resonators in-situ without disturbing the main mode is demonstrated and is a crucial step towards a robust fielded widely tunable filter.**

***Index Terms* —Cavity resonators, evanescent-mode filters, tunable filters, piezoelectric transducers, frequency control.**

I. Introduction

The recent trend in microwave systems is to enable adaptable and dynamically reconfigurable communication systems, such as software defined and cognitive radios where baseband processing is done using digital techniques [1]. The spectrum of interest therefore is generally very wide however this makes the receiver susceptible to interferers that could saturate the system. Ideally, the waveform could be isolated by a preselect filter, however this filter would have to be widely tunable. Furthermore, in order to do band- or even channel-selection prior to the low-noise amplifier (LNA) the filter needs to have a very low loss in order to maintain a reasonable noise figure for the system. The need for low loss combined with narrow bandwidth dictates that the quality factor (Q) of the filter needs to be very high.

Tunable filter research has been increasing and several technologies have been shown to be able to provide tunable filters, such as microelectromechanical systems (MEMS) [2], [3] and ferroelectric thin films [4]. Microstrip resonators have also been tuned using piezoelectric transducers and commercially available varactors [5], [6]. However, none of these methods provide simultaneously a high-Q and wide tuning range.

Evanescent-mode cavity resonators have been demonstrated to satisfy these requirements [7], [8]. Filters constructed out of two high-Q evanescent-mode cavities have been reported with narrow bandwidths while maintaining a low loss [9]. A filter with a 0.5% bandwidth at 4.72 GHz was also shown where piezoelectric actuators were used to compensate for fabrication tolerances [9]. Such narrow bandwidths require fine tuning of the resonators.

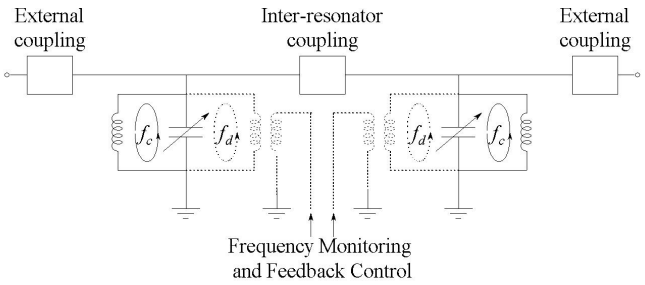

Fig. 1. A block diagram of a two pole tunable filter with frequency monitoring and feedback control where the differential mode frequency, f_d, is monitored independently from the common mode center frequency of each resonator, f_c. The dotted lined monitoring networks are not seen by the filter but the tunable capacitor is used by both the modes.

The cavities are extremely frequency sensitive to any change in the capacitive gap between the post and the top of the cavity. This enables the extreme tuning ranges of the widely tunable evanescent-mode cavity filters. However, this sensitivity also makes the filters vulnerable to environmental effects such as temperature changes which can cause slight geometrical changes due to the thermal expansion or contraction of the actuators used. Because the entire tuning is done with only tens of microns of displacement this geometrical change can potentially cause large frequency shifts. In addition, piezoelectric actuators generally exhibit some hysteresis which prevents the use of a simple voltage look-up table to control the filters. An in-situ closed loop feedback control is highly desirable to automatically compensate for any detuning of the filter, particularly for very narrow band filters.

Several methods have been reported for tuning filters such as using a time-domain transformation of the return loss [10] and more recently using fuzzy logic [11]. These methods all require direct measurement of the input and/or the output of the filter and can not be done while the filter is in operation or in the field.

In this paper, an in-situ method for tracking the center frequency of a tunable evanescent-mode cavity filter is presented. This method continuously monitors the common mode frequency of each resonator independently by using higher order differential modes. These modes are created by splitting the capacitive post of the resonator. A block diagram of a tunable filter with an in-situ monitoring is shown in Fig. 1.

The ratio between the differential mode and the center frequency of the filter is derived to provide guidelines for designing a specific frequency separation between the two modes. There is a unique correspondence between the differential mode and the resonant frequency of each of the resonators. A filter is fabricated to demonstrate the concept and tuned over a range greater than an octave by controlling the higher order differential mode.

II. Theory

In order to understand the relationship between the center frequency of the filter and the frequency of the higher order differential mode for monitoring of an evanescent-mode cavity resonator such as shown in Fig. 2, an equation relating the ratio of the frequencies to the physical dimensions of the resonator is desirable. In Fig. 2 (d) the orientation and magnitude of the magnetic field is shown for a post that is split into two equal sections. The magnetic field of the differential mode is at a maximum in the volume between the two posts while the magnetic field of the common mode is at a minimum allowing for a monitoring port at this location that does not disturb the common mode. The symmetry of the differential mode in the cavity can be utilized to prevent coupling of the differential mode out of the filter ports by locating them the evenly on symmetry plane. This in effect isolates the differntial mode of each resonator. However, they share the same capacitive region in the cavity and this allows the differential mode to accurately monitor the common mode of the resonators in the filter.

Looking at an evanescent-mode resonator, such as shown in Fig. 2, the resonant frequencies of the two modes can be estimated. First the differential mode frequency is found using some assumptions. The first assumption is that the gap (g) is much smaller than the cavity height (h) as is required for the sensitive tuning. This causes the electric field to be uniform above the post when neglecting the fringing fields. Using the electric field the total charge (Q) on each post top (area of A_p) can be calculated and related to the current (I) on the post walls. The magnetic field concentration inside the split post is much higher than in the rest of the cavity and therefore another approximation made is that all the current is flowing on the walls inside of the post. The magnetic field in the split post can then be calculated from the current density on the post wall.

The energy stored in the electric and magnetic fields can then be found and related to the spacing between the two halves of the post (w) and length (L) of the split post.

$$W_e = \frac{1}{4}\varepsilon \iiint_V \left|\vec{E}\right|^2 dV = \frac{1}{2}\varepsilon A_p g E_0^2 \qquad (1)$$

$$W_m = \frac{1}{4}\mu \iiint_V \left|\vec{H}\right|^2 dV = \frac{\mu h w \varepsilon^2 E_0^2 \omega^2 A_p^2}{4L} \qquad (2)$$

Equating the two at resonance to find the resonant frequency of the higher order differential mode, f_d,

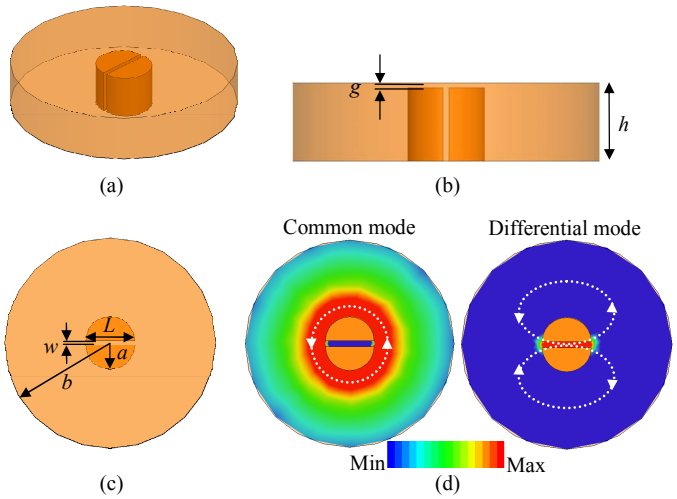

Fig. 2. Schematic of an evanescent-mode cavity with a split post, (a) 3D view, (b) cross-section, (c) top view, and (d) magnetic field of both the common and differential modes.

$$W_e = W_m \rightarrow f_d = \frac{1}{2\pi}\sqrt{\frac{2gL}{\mu\varepsilon h w A_p}}, \qquad (3)$$

which for the case in Fig. 2 where the post is made of a split cylindrical post the area A_p is $\pi a^2/2$ and the length L is $2a$ the equation for the frequency becomes

$$f_d = \frac{1}{2\pi}\sqrt{\frac{8g}{\mu\varepsilon h w \pi a}}. \qquad (4)$$

Next the common mode frequency is estimated by approximating the cavity inductance as the inductance of a coaxial line section and the cavity capacitance as the parallel plate capacitance between the top of the post and the top of the cavity, which is a fair assumption for very small gaps. The frequency of the common mode, f_c, can then be calculated.

$$f_c = \frac{1}{2\pi}\sqrt{\frac{1}{LC}} = \frac{1}{2\pi}\sqrt{\frac{2g}{\mu\varepsilon a^2 \ln(b/a) h}} \qquad (5)$$

An HFSS eigenmode simulation is used to validate (4) and (5), the comparison is shown in Fig. 3, the theoretical frequencies agree well with the simulated ones. And finally the ratio of the two frequencies can be estimated using

$$R_{d-c} = \frac{f_d}{f_c} \approx 2\sqrt{\frac{a\ln(b/a)}{\pi w}}. \qquad (6)$$

This equation gives the design guidelines for choosing the desired frequency ratio, though derived with approximations. The equation works for a range of frequencies and can be used as a useful starting point for designing the differential mode. Practical implementations such as shown below may not have the identical relationships as described by (6) because of the integrated substrate method of realizing the cavities with vias instead of complete walls. However, the analytical formula is

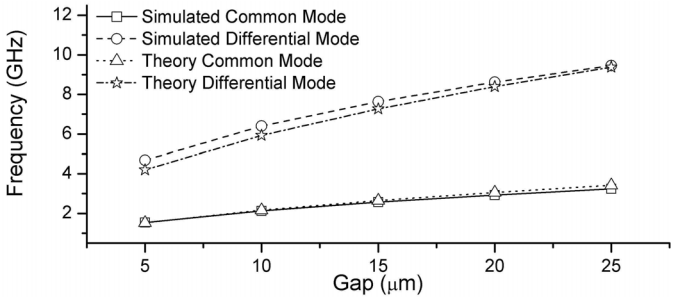

Fig. 3. Comparison between the simulated and theoretical frequencies of the common and differential modes.

a useful analysis to demonstrate the expected ratio and the physics of the operation of the modes that were implemented. The assumptions are stretched when the frequency of the differential mode becomes high enough that the height of the cavity is large relative to wavelength and when the spacing between the two post halves becomes too large and the magnetic field in the slot is no longer much greater than the field in the cavity outside of the post.

III. Measurement and Analysis

In order to verify the monitoring capabilities of the in-situ differential mode tracking method a two pole filter was designed. The filter consists of a double sided Rogers TMM3 circuit board and via cages are used to create the resonators, inter-resonator coupling, and the posts. The posts are formed by four copper thru vias and the top metal is split down the middle with a 0.25 mm gap, which is created by simple etching of the top substrate as shown in Fig. 4 (a). The post vias are 1.2 mm apart. A coupling aperture is created in the bottom copper and a shorted coplanar waveguide (CPW) feed line forms probe pads for monitoring the differential mode frequency. The location of the aperture is in the center of the resonator to prevent any disturbances to the common mode. The aperture is chosen to be as large as permittable by the post vias. This will ensure maximum magnetic field coupling. The CPW line width and the gaps are all 0.2 mm. A close up of the split post and the CPW monitoring line is shown in Fig. 4 (b).

The filter was fabricated using a traditional circuit board plotter. The first step was to drill the post vias and metallize them. Then a 35 μm copper foil was laminated on the top face of the circuit board to form the top of the cavity, Fig. 4 (c) shows a cross-section of the post area. Vias are then drilled through both the substrate and the copper foil and electroplated, creating a high quality electrical connection to the top of the cavity. Piezoelectric disc actuators are attached to the top of the copper foil using silver epoxy to provide the tunability of the filter.

Probes were used to measure the differential modes, while the filter was measured independently using a separate network analyzer. The common modes of the resonators are first swept across the range of tunable frequencies and the correspondence between the differential mode and the

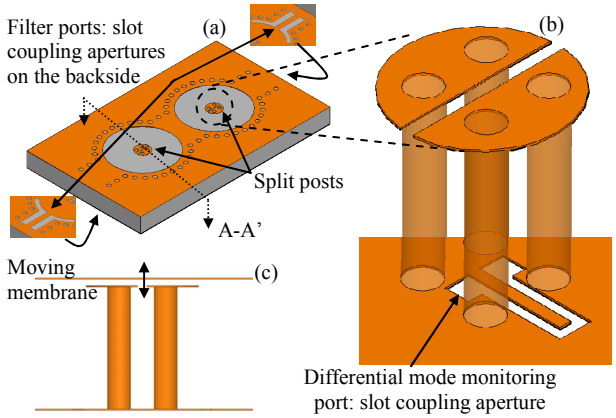

Fig. 4. HFSS model of the fabricated tunable evanescent-mode filter with the split posts for frequency monitoring, (a) view of the top metal layer, (b) close up of the split post showing the CPW monitoring line on the bottom metal layer, and (c) A-A' cross-section of the split post showing the moving copper membrane.

common mode is recorded as show in Fig. 5. There are slight variations in the correspondence of the two modes based on fabrication imperfections such as in the angle of depression of the membrane, however the correlation is unique for each resonator.

The differential modes were then used exclusively to tune the filter into the desired frequency ranges and filter shape. The resonance of the differential mode was monitored by a network analyzer. The information was then fed via GPIB into a LABVIEW control program, which handles the piezoelectric voltage control thus providing a fully automated feedback loop that can tune the filter in a matter of seconds. This feedback mechanism could be replaced by an independent oscillator, for example.

An example of using the differential modes to tune a filter is shown in Fig. 6, where the two differential modes are moved to the frequencies of 6.56 and 6.48 GHz using the data from Fig. 5. This causes the common modes to align to 3.04 GHz

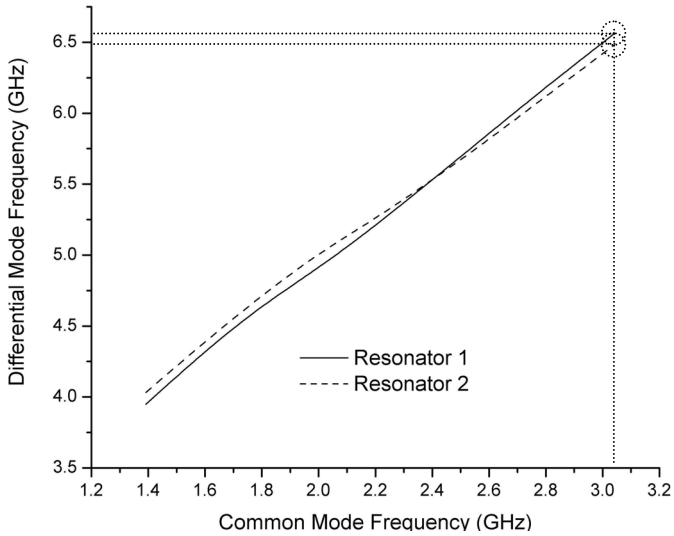

Fig. 5. Measured relationship between the center frequency of the filter and the higher order mode of each resonator.

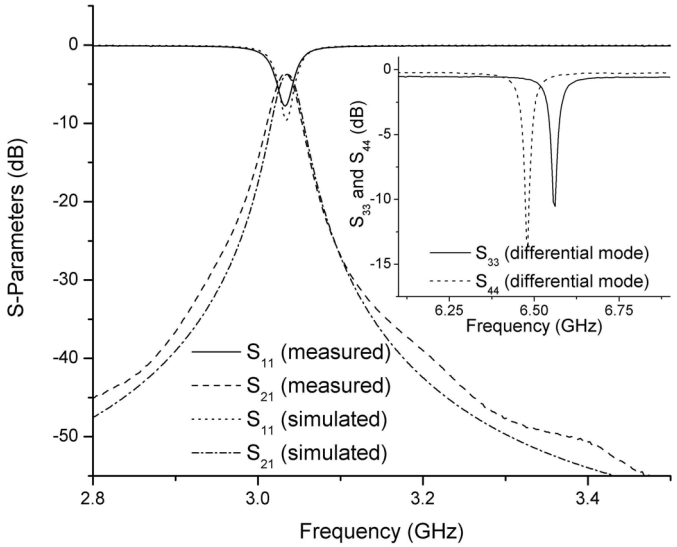

Fig. 6. Simulated and measured response of a 0.9% filter at 3.04 GHz with the measured differential monitoring modes shown in the inset.

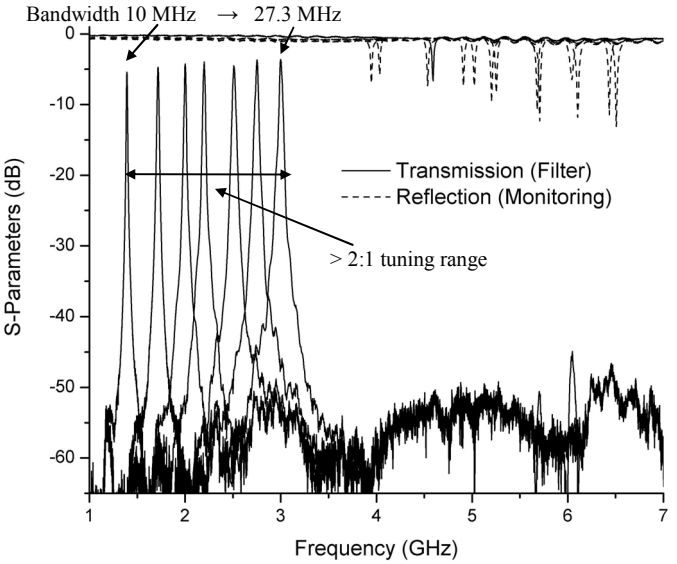

Fig. 7. Measured filter tuning from 1.4 to 3 GHz along with the higher order differential modes used for tuning.

forming the filter shape dictated by the inter-resonator coupling and not by an offset in resonator frequency. It is very difficult to align both resonators to exactly the same frequency without feedback. The measured insertion loss is 3.43 dB and the 3 dB bandwidth is 27.3 MHz. The expected insertion loss from simulation is 3.10 dB with a 3 dB bandwidth of 24.6 MHz. Fig. 6 shows the comparison between the simulation and the measurement, which are in good agreement showing that the loss and matching are as expected. This was repeated across the 1.4 to 3 GHz tuning range of the filter and the performance is shown in Fig. 7. The achieved 3 dB filter bandwidth was as low as 10 MHz (0.7% fractional bandwidth) at the low end and as high as 27.3 MHz (0.9% fractional bandwidth) at the high end. The monitoring of the higher order differential mode that was used to perform the tuning is also shown. The out of band rejection of the filter is better than 45 dB over the entire range of the differential mode.

IV. Conclusion

A method for in-situ monitoring of the center frequency of a widely tunable evanescent-mode cavity filter using a differential mode generated by splitting the capacitive post in two was presented. The frequency of the differential mode of each resonator was independently mapped to their common mode frequencies. This mapping is then used to automatically tune the filter without using the signal path through the filter. A filter with monitoring was tuned from 1.4 to 3 GHz. This monitoring technique is a crucial step towards enabling robust, widely tunable filters.

Acknowledgement

This work was supported by the DARPA Analog Spectral Processors (ASP) project.

References

[1] W. H. W. Tuttlebee, "Software-defined radio: Facets of a developing technology," *IEEE Personal Commun. Mag.*, vol. 6, pp. 38-44, Apr. 1999.

[2] D. Peroulis, S. Pacheco, K. Sarabandi, and L. P. B. Katehi, "Tunable lumped components with applications to reconfigurable MEMS filters," *IEEE MTT-S Int. Microwave Symp. Dig*., vol. 1, pp. 341-344, 2001.

[3] W. D. Yan and R. R. Mansour, "Tunable Dielectric Resonator Bandpass Filter With Embedded MEMS Tuning Elements," *IEEE Trans. Microw. Theory Tech.*, vol. 55, no. 1, pp. 154-160, Jan. 2007.

[4] A. T. Findikoglu, Q. X. Jia, X. D. Wu, G. J. Chen, T. Venkatesan, and D. W. Reagor, "Tunable and adaptive bandpass filter using a nonlinear dielectric thin film of SrTiO3," *Appl. Phys. Lett*., vol. 68, no. 12, pp. 1651-1653, 1996.

[5] M. Al-Ahmad, R. Maenner, R. Matz, and P. Russer, "Wide piezoelectric tuning of LTCC bandpass filters," *IEEE MTT-S Int. Microwave Symp. Dig*., vol. 4, pp. 1275-1278, 2005.

[6] A. R. Brown and G. M. Rebeiz, "A varactor-tuned RF filter," *IEEE Trans. Microw. Theory Tech.*, vol. 48, no. 7, pp. 1157-1160, July 2000.

[7] J. R. White, C. J. White, and A. H. Slocum, "Octave-tunable miniature RF resonators," *IEEE Microwave Wireless Compon. Lett.,* vol. 15, no. 11, pp. 793-795, Nov. 2005.

[8] S. Hajela, X. Gong, and W. J. Chappell, "Widely Tunable High-*Q* Evanescent-Mode Resonators Using Flexible Polymer Substrates," *IEEE MTT-S Int. Microwave Symp. Dig.*, vol. 4, pp. 2139-2142, 2005.

[9] H. Joshi, H. H. Sigmarsson, D. Peroulis, and W. J. Chappell, "Highly Loaded Evanescent Cavities for Widely Tunable High-Q Filters," *IEEE MTT-S Int. Microwave Symp. Dig.*, pp. 2133-2136, 3-8 June 2007.

[10] J. Dunsmore, "Tuning band pass filters in the time domain," *IEEE MTT-S Int. Microwave Symp. Dig.*, vol. 3, pp. 1351-1354, 1999.

[11] V. Miraftab and R. R. Mansour, "Computer-aided tuning of microwave filters using fuzzy logic," in *IEEE MTT-S Int. Microwave Symp. Dig.*, vol. 2, pp. 1117-1120, 2002.